A molecular mechanism for aberrant CFTR-dependent HCO_3^- transport in cystic fibrosis

Shigeru B.H.Ko[1,2], Nikolay Shcheynikov[1], Joo Young Choi[1], Xiang Luo[1], Kenichi Ishibashi[3], Philip J.Thomas[1], Joo Young Kim[4], Kyung Hwan Kim[4], Min Goo Lee[4], Satoru Naruse[2,5] and Shmuel Muallem[1,5]

[1]Department of Physiology, UT Southwestern Medical Center, Dallas, TX 75390, USA, [2]Department of Internal Medicine II, Nagoya University School of Medicine, Nagoya 466-8550, [3]Department of Pharmacology, Jichi Medical School, Tochigi-ken, Japan and [4]Department of Pharmacology, Yonsei University, Seoul 120-752, Korea

[5]Corresponding authors
e-mail: Shmuel.Muallem@UTSouthwestern.edu or
snaruse@med.nagoya-u.ac.jp

S.B.H.Ko, N.Shcheynikov and J.Y.Choi contributed equally to this work

Aberrant HCO_3^- transport is a hallmark of cystic fibrosis (CF) and is associated with aberrant Cl^--dependent HCO_3^- transport by the cystic fibrosis transmembrane conductance regulator (CFTR). We show here that HCO_3^- current by CFTR cannot account for CFTR-activated HCO_3^- transport and that CFTR does not activate AE1–AE4. In contrast, CFTR markedly activates Cl^- and OH^-/HCO_3^- transport by members of the SLC26 family DRA, SLC26A6 and pendrin. Most notably, the SLC26s are electrogenic transporters with isoform-specific stoichiometries. DRA activity occurred at a Cl^-/HCO_3^- ratio $\geqslant 2$. SLC26A6 activity is voltage regulated and occurred at $HCO_3^-/Cl^- \geqslant 2$. The physiological significance of these findings is demonstrated by interaction of CFTR and DRA in the mouse pancreas and an altered activation of DRA by the R117H and G551D mutants of CFTR. These findings provide a molecular mechanism for epithelial HCO_3^- transport (one SLC26 transporter—electrogenic transport; two SLC26 transporters with opposite stoichiometry in the same membrane domain—electroneutral transport), the CF-associated aberrant HCO_3^- transport, and reveal a new function of CFTR with clinical implications for CF and congenital chloride diarrhea.
Keywords: CFTR/cystic fibrosis/electrogenic Cl^-/HCO_3^- transporters/SLC26

Introduction

Many cystic fibrosis transmembrane conductance regulator (CFTR)-expressing epithelia secrete copious amounts of HCO_3^- (Argent and Case, 1994; Cook *et al.*, 1994; Quinton, 1999). HCO_3^- is an ion with particular physiological importance, as it is the biological pH buffer and it affects the solubility of macromolecules and ions in biological fluids. Aberrant HCO_3^- secretion has long been associated with cystic fibrosis (CF), in particular with the pancreatic status of the patients (Johansen *et al.*, 1968; Kopelman *et al.*, 1988; Kristidis *et al.*, 1992). Furthermore, in a recent work, we demonstrated that many CF-associated mutations in CFTR affect CFTR-activated HCO_3^- transport more than Cl^- transport (Choi *et al.*, 2001). Hence, understanding the mechanisms of HCO_3^- secretion is of particular significance with respect to CF.

Epithelial HCO_3^- transport has electrogenic and electroneutral components, the contribution of which is tissue specific. Although the involvement of CFTR in HCO_3^- transport has been established unequivocally, how CFTR regulates each component of HCO_3^- secretion is unknown. When expressed in heterologous systems, CFTR can function as a Cl^- and HCO_3^- channel (Poulsen *et al.*, 1994; Linsdell *et al.*, 1997; O'Reilly *et al.*, 2000). Therefore, it is generally assumed that CFTR itself mediates the electrogenic component of HCO_3^- transport. The electroneutral component is thought to be mediated by a Cl^-/HCO_3^- exchanger. CFTR may regulate all forms of HCO_3^- secretion, since Cl^--dependent HCO_3^- transport is reduced in the pancreatic and submandibular gland (SMG) ducts of ΔF508 mice (ΔF) (Lee *et al.*, 1999b).

In spite of its importance in CF, the proteins mediating HCO_3^- transport and their regulation by CFTR are not known. CFTR could activate one of the SLC4 anion exchangers (Alper, 1991) or one of the newly discovered SLC26 anion transporters (Lohi *et al.*, 2000). Members of the family include down-regulated in adenoma/congenital chloride diarrhea (DRA) (Moseley *et al.*, 1999), pendrin (Everett *et al.*, 1997) and SLC26A6 (Knauf *et al.*, 2001). DRA functions as a Cl^-/OH^- and Cl^-/HCO_3^- exchanger (Melvin *et al.*, 1999), pendrin functions as a Cl^-/OH^-, Cl^-/HCO_3^- and $Cl^-/formate$ exchanger (Soleimani *et al.*, 2001), whereas SLC26A6 functions as a $Cl^-/formate$ (Knauf *et al.*, 2001) and Cl^-/HCO_3^- exchanger (Wang *et al.*, 2002). Alternatively, CFTR itself could mediate all forms of HCO_3^- transport. In the present work, we measured net Cl^- and HCO_3^- fluxes, and membrane potential and current in *Xenopus* oocytes and HEK 293 cells, to show that the SLC26s are electrogenic Cl^- and HCO_3^- transporters with isoform-specific stoichiometries. Most notably, CFTR markedly activates members of the SLC26 family tested, which was compromised by mutations in CFTR associated with CF. Activation of only one SLC26 transporter or two transporters with opposite stoichiometries can account for activation of all forms of epithelial HCO_3^- transport by CFTR. These findings provide a molecular mechanism for aberrant HCO_3^- transport in CF.

Results and discussion

CFTR activates Cl^--dependent HCO_3^- transport
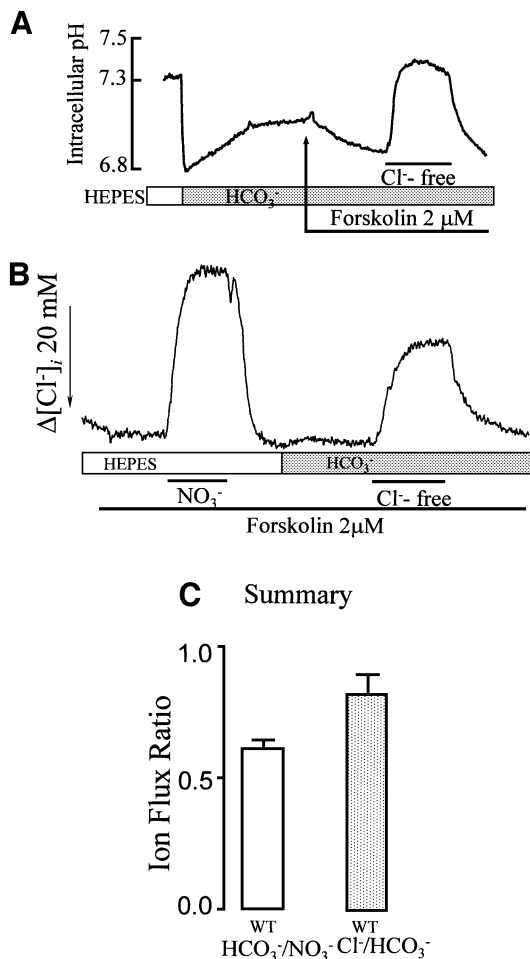HCO_3^- transport activated by CFTR can occur as a coupled, electroneutral Cl^-/HCO_3^- exchange or as Cl^- and

Fig. 1. Cl$^-$ and HCO$_3^-$ transport in CFTR-expressing HEK 293 cells. (**A**) pH$_i$ measurement: CFTR-transfected cells were incubated in HCO$_3^-$-buffered solutions as indicated. After stabilization of pH$_i$, the cells were stimulated with forskolin and transiently exposed to a Cl$^-$-free medium. (**B**) [Cl$^-$]$_i$ measurements: cells expressing CFTR and loaded with MQAE were perfused with HEPES-buffered solutions to measure Cl$^-$/NO$_3^-$ exchange and then in HCO$_3^-$-buffered solutions to measure Cl$^-$/HCO$_3^-$ exchange. For measurement of Cl$^-$/NO$_3^-$ exchange, Cl$^-$ was replaced with NO$_3^-$. (**C**) Flux ratio: to calculate the flux ratios, the rates of [Cl$^-$]$_i$ changes due to incubating the same cells with NO$_3^-$ (HEPES, first portion of trace in B) or Cl$^-$-free gluconate solution (HCO$_3^-$, second portion of trace in B) were calculated and used to obtain the HCO$_3^-$/NO$_3^-$ ratio. The average is from nine similar experiments. The Cl$^-$/HCO$_3^-$ ratio was calculated from measurement of pH$_i$ (A) and accounting for the buffer capacity, and the measurement of Cl$^-$ transport with MQAE, as in the second portion of (B). The number of pH$_i$ and [Cl$^-$]$_i$ experiments averaged is five and nine, respectively.

HCO$_3^-$ currents. In a previous work, we showed that HCO$_3^-$ transport was dependent on Cl$^-$ and was not inhibited by depolarizing the cells with high external K$^+$ (Lee *et al.*, 1999a). To understand better the mechanism of CFTR-activated HCO$_3^-$ transport, we first measured HCO$_3^-$ and Cl$^-$ fluxes under the same conditions. HCO$_3^-$ flux was estimated from changes in pH$_i$, and [Cl$^-$]$_i$ was measured with N-(6-methoxyquinolyl) acetoethyl ester (MQAE). Figure 1A shows that exposing the cells to a HCO$_3^-$-buffered solution resulted in the typical acidification due to hydration of CO$_2$ and partial recovery of pH$_i$ by Na$^+$/H$^+$ exchange and Na$^+$-HCO$_3^-$ co-transport. pH$_i$ then stabilized at 7.13 $\pm$ 0.03 ($n = 9$). After stimulation with
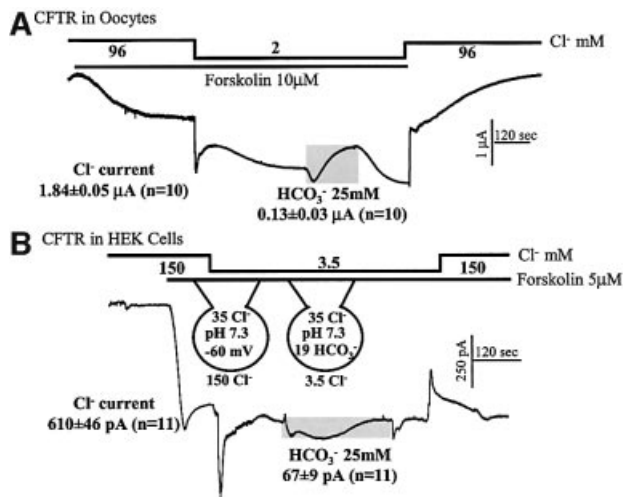

Fig. 2. Macroscopic Cl$^-$ and HCO$_3^-$ currents in *Xenopus* oocytes and HEK 293 cells expressing CFTR. (**A**) Oocytes were injected with water (controls) or cRNA coding for CFTR. Water-injected oocytes ($n = 15$) never showed forskolin-activated Cl$^-$ current, and all cRNA injected oocytes ($n = 10$) showed such a current. Oocytes were stimulated with 10 μM forskolin to activate CFTR. After the current reached steady state, 94 mM Cl$^-$ was replaced with gluconate and then 25 mM gluconate was replaced with 25 mM HCO$_3^-$. The duration of incubation with HCO$_3^-$ is marked by the gray bar. The average of Cl$^-$ and HCO$_3^-$ currents from 10 experiments is given in the figure and the text. (**B**) Cl$^-$ and HCO$_3^-$ currents in HEK 293 cells. After establishing the whole-cell configuration, HEK 293 cells transfected with CFTR were perfused with a HEPES-buffered solution containing 150 mM NMDG-Cl. The cells were then stimulated with forskolin before ($n = 6$) or after ($n = 5$) exposure to 3.5 mM Cl$^-$. After the current stabilized, the cells were incubated with solutions buffered with 25 mM HCO$_3^-$ while maintaining constant external [Cl$^-$]. After stabilization of the current, HCO$_3^-$ was removed by perfusing with HEPES-buffered solutions. The currents mediated by CFTR recorded under each condition were averaged and are presented as the means $\pm$ SEM of the number of experiments listed in parentheses.

forskolin, removal and addition of Cl$^-$ resulted in the expected pH$_i$ increase and decrease. Figure 1B shows measurement of [Cl$^-$]$_i$ with MQAE to estimate both conductive and HCO$_3^-$-driven Cl$^-$ fluxes in the same cells. Conductive fluxes were estimated from measurement of Cl$^-$/NO$_3^-$ exchange (Choi *et al.*, 2001) since CFTR conducts NO$_3^-$ better than Cl$^-$ (Linsdell *et al.*, 1997). HCO$_3^-$-driven Cl$^-$ transport was measured by incubating the cells with HCO$_3^-$ and replacing Cl$^-$ with gluconate. CFTR does not conduct gluconate and, under these conditions, Cl$^-$ transport is dependent on HCO$_3^-$ transport. Measurement of [Cl$^-$]$_i$ under both conditions allowed the HCO$_3^-$/NO$_3^-$ flux ratio to be estimated. Figure 1C shows that this ratio is ~0.65, higher than expected from the relative permeability of CFTR to Cl$^-$ and HCO$_3^-$ (~0.1). Estimating net HCO$_3^-$ influx from the increase in pH$_i$ (Figure 1A) and net Cl$^-$ efflux from the decrease in [Cl$^-$]$_i$ (Figure 1B), we calculated a Cl$^-$/HCO$_3^-$ flux ratio of close to 1 (Figure 1C). This ratio indicates similar net Cl$^-$ and HCO$_3^-$ fluxes by the CFTR-activated mechanism(s).

The HCO$_3^-$/NO$_3^-$ ratio provided the initial clue that HCO$_3^-$ current by CFTR cannot account for the HCO$_3^-$ fluxes. To estimate further the contribution of HCO$_3^-$ current, we measured Cl$^-$ and HCO$_3^-$ currents in cells expressing CFTR under the experimental conditions used
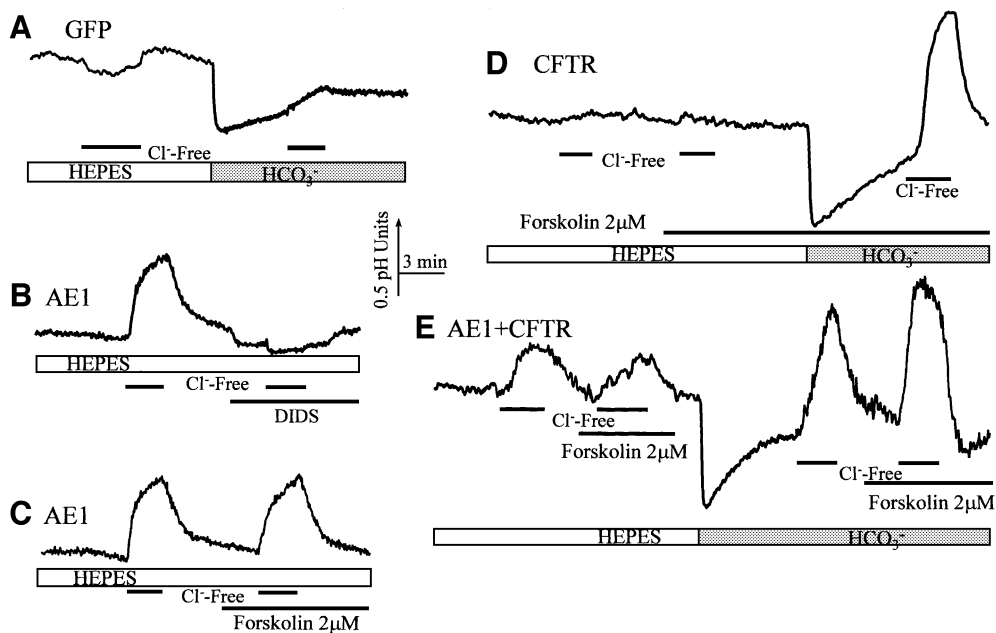
Fig. 3. CFTR does not activate the SLC4 exchangers. The figure shows only experiments performed with AE1; a similar lack of activation by CFTR of AE2, AE3 and AE4 was observed. HEK 293 cells were transfected with GFP (A; *n* >10), AE1 (B and C; *n* = 8), CFTR (D; *n* >10) or AE1 and CFTR (E; *n* = 6). Cl^-/OH^- and Cl^-/HCO_3^- exchange were measured by exposing the cells to Cl^--free media in solutions buffered with HEPES or HCO_3^-, respectively. In (**A**), the lack of measurable Cl^-/OH^- and minimal Cl^-/HCO_3^- exchange activity in control cells is shown. It can be seen in (**B**) that AE1 has DIDS-inhibitable Cl^-/OH^- exchange activity and in (**C**) that AE1 activity is not stimulated by forskolin. In (**D**), it is shown that activated CFTR alone does not activate a large Cl^-/OH^- exchange, and in (**E**) that neither AE1-mediated Cl^-/OH^- nor Cl^-/HCO_3^- exchange are activated by CFTR.

to measure pH_i and $[Cl^-]_i$. First, we compared Cl^- and HCO_3^- currents by CFTR expressed in *Xenopus* oocytes (Figure 2A). Stimulation of CFTR in oocytes held at –50 mV and bathed in 96 mM Cl^- resulted in the expected inward current. Reducing external Cl^- to 2 mM caused a rapid, but partially transient increase in inward current, which then stabilized at 1.84 ± 0.05 µA. The transient may reflect the dependence of Cl^- current on $[Cl^-]_o$, as was reported for other Cl^- channels (Pusch *et al.*, 1999). Subsequent exposure of the oocytes to 25 mM HCO_3^- increased the inward current by only 0.13 ± 0.03 µA and then the current partially inactivated. At a membrane potential of –50 mV, an inward HCO_3^- current is expected due to accumulation of HCO_3^- in the oocytes. The inactivation probably reflects inhibition of CFTR Cl^- current by HCO_3^- (O'Reilly *et al.*, 2000). Removal of HCO_3^- restored the Cl^- current, and addition of external Cl^- resulted in the expected reduction in inward current. These measurements show that at physiological $[HCO_3^-]$ the CFTR-mediated HCO_3^-/Cl^- current ratio is only 0.07, dramatically different from the flux ratio of 0.65 shown in Figure 1C.

The measurements in oocytes may not reflect the behavior of CFTR in mammalian cells. In addition, it is difficult to estimate net Cl^- and HCO_3^- fluxes from the current in oocytes. Therefore, we performed similar experiments in CFTR-transfected HEK 293 cells where we can obtain all parameters needed for such calculations (Figure 2B). The cells were dialyzed internally with a solution containing 35 mM Cl^-, pH 7.3 and bathed in a solution containing 150 mM *N*-methyl D-glucamine (NMDG)-Cl, pH 7.4. The membrane potential was held at –60 mV. The only permeable ion under these conditions

is Cl^-, and the Cl^- and pH gradients are similar to those of resting cells. Stimulation with forskolin activated a Cl^- current. Reducing bath Cl^- to 3.5 mM resulted in a transient increase in inward current that then stabilized at 610 ± 46 pA ($n = 11$). Again, the transient may reflect gating of Cl^- current by external Cl^- (Pusch *et al.*, 1999). Addition of HCO_3^- caused a variable outward current, which was followed by an inward current that peaked at 67 ± 9 pA ($n = 11$). A HCO_3^--dependent inward current is expected from establishment of a 19 mM $[HCO_3^-]_i$/25 mM $[HCO_3^-]_o$ gradient. $[HCO_3^-]_i$ was calculated by the Henderson–Hasselbalch equation using a pH_i of 7.3 and 5% CO_2. Removal of HCO_3^- resulted in a transient inward current, as expected from the transient increase in outward HCO_3^- gradient and removal of inhibition by HCO_3^-.

The peak HCO_3^- current measured at low external Cl^- can account for at most 30% of the Cl^--dependent HCO_3^- flux. Thus, a current of 67 pA corresponds to a transport of $67 \times (6 \times 10^6) \times 60 = 2.41 \times 10^{10}$ ions/min. From an averaged cell capacitance of 13.1 ± 0.4 pF, we calculate a cell radius of 10.21 µm and a cell volume of 4.45 pl. Therefore, the HCO_3^- current can generate a flux of 9.03 mM/min. The net HCO_3^- flux calculated from the change in pH_i and the buffer capacity is (0.76 ΔpH units/min $\times$ 41.3 βt) 31.4 mM/min.

The findings in Figures 1 and 2 led us to conclude that CFTR itself is not likely to mediate the bulk of the HCO_3^- transport observed in HEK 293 cells expressing CFTR. Thus, the HCO_3^-/Cl^- (NO_3^-) flux ratio is higher than the HCO_3^-/Cl^- permeability ratio of CFTR, and the HCO_3^- current cannot account for the HCO_3^- flux. Therefore, it appears that in addition to its function as a Cl^- channel, CFTR activates other Cl^-/HCO_3^- transporters.
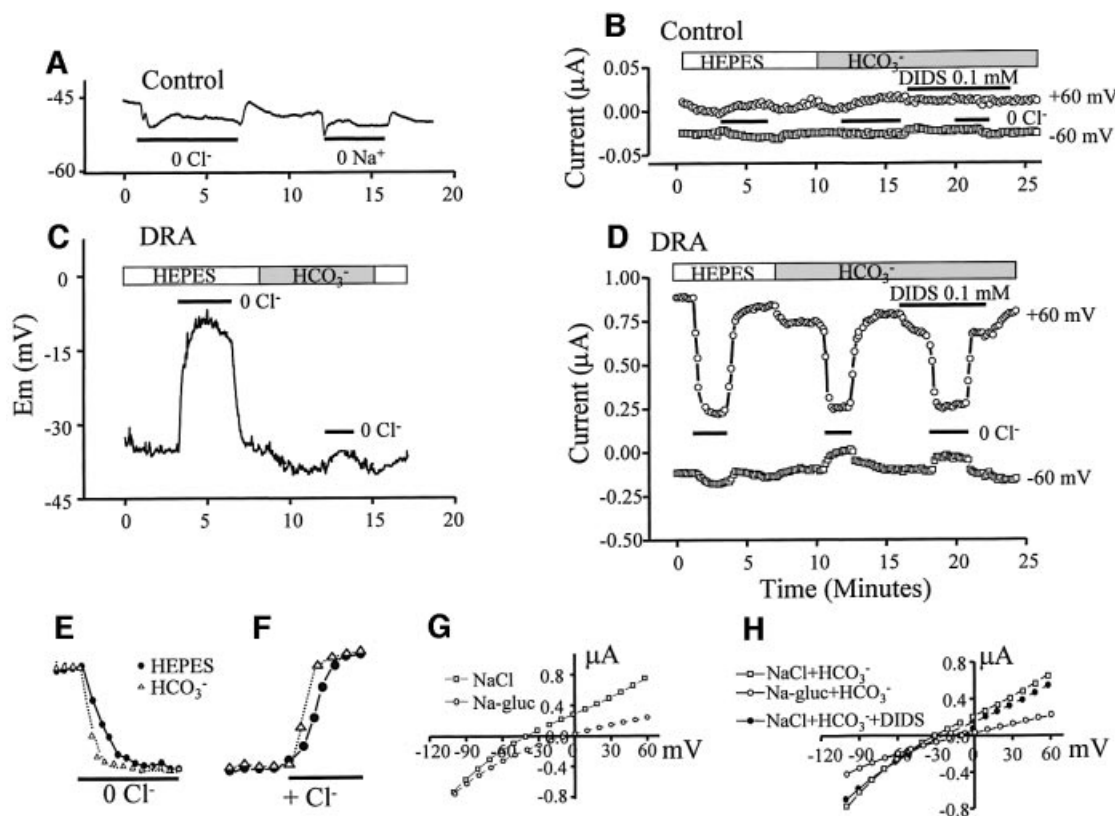
Fig. 4. Electrogenic Cl^- and HCO_3^- transport by DRA. Control oocytes (A and B) or those expressing DRA (C–H) were used to measure MP (**A** and **C**), current (**B** and **D**), the rate of current changes (**E** and **F**) or *I–V* relationships (**G** and **H**). As indicated by the bars, the oocytes were incubated in Cl^--free solutions in the absence (open bars) or presence (gray bar) of HCO_3^-. Where indicated in (B) and (D), the oocytes were exposed to 0.1 mM DIDS. Current was measured at a holding MP of –30 mV and stepping to ±60 mV every 10 s for 0.5 s. The *I–V* plots were recorded after stabilization of the MP following solution changes by holding the MP at 0 mV for 500 ms between steps and stepping from –100 to +80 for 250 ms at 10 mV intervals. The plots in (G) and (H) are typical of six to eight separate experiments.

In the next phase of the studies, we set out to establish the molecular identity of the Cl^-/HCO_3^- transporters.

CFTR does not activate the SLC4 transporters

An obvious possibility is that CFTR activates members of the SLC4 Cl^-/HCO_3^- exchangers AE1–AE4. To test this possibility, we co-expressed CFTR with AE1, AE2, AE3 or AE4 and measured the effect of CFTR on their activity. The protocols used to test the effect of CFTR on the AEs are shown in Figure 3 for AE1. The results with AE1 are shown because, when expressed, AE1 resides in the luminal membrane of epithelia (Sabolic *et al.*, 1997). In these experiments, we relied on the ability of all AEs, but not of CFTR, to mediate Cl^-/OH^- exchange. Figure 3A shows that control cells have no Cl^-/OH^- and low Cl^-/HCO_3^- exchange activity. The Cl^-/HCO_3^- exchange activity in control cells probably originates from low levels of SLC26 members. RT–PCR revealed that the HEK 293 clone used in this work has low levels of mRNA for SLC26A7 and two splice variants of SLC26A9. This can also account for activation of Cl^--dependent HCO_3^- transport in cells transfected with CFTR only (Figure 3D). The low levels of the SLC26 members was probably not sufficient to see the Cl^-/OH^- exchange activity in control cells.

Figure 3B shows that transfecting cells with AE1 gave rise to a robust Cl^-/OH^- exchange that was inhibited by the AEs inhibitor DIDS. Figure 3C shows that Cl^-/OH^-

exchange activity by AE1 is not stimulated by forskolin. The final control in Figure 3D shows that stimulation of CFTR activated Cl^-/HCO_3^-, but not Cl^-/OH^-, exchange activity. Figure 3E shows the results obtained in cells transfected with both CFTR and AE1. Activation of CFTR had no effect on Cl^-/OH^- (HEPES) or Cl^-/HCO_3^- (HCO_3^-) exchange activity of AE1. The activity measured in the presence of HCO_3^- is close to the sum of the activities measured by expression of the individual proteins. The experiments in Figure 3 were performed with cells transfected with low levels of AE1. A similar lack of effect of CFTR on AE activity was also obtained in cells transfected with CFTR and low and high levels of AE1, AE2, AE3 or AE4 (not shown), excluding the possibility that a lack of effect is due to low protein levels. These results indicate that CFTR does not activate any of the known SLC4 isoforms.

Members of the SLC26 family are electrogenic Cl^- and HCO_3^- transporters

A newly discovered family of Cl^- and HCO_3^- transporters is SLC26 (Lohi *et al.*, 2000). Three members of the family, DRA (Melvin *et al.*, 1999), PDS (Soleimani *et al.*, 2001) and SLC26A6 (Wang *et al.*, 2002), were reported to function as Cl^-/HCO_3^- exchangers and are expressed in the luminal membrane of epithelia. Therefore, they could be the transporters stimulated by CFTR. Before testing their interaction with CFTR, we examined Cl^- and HCO_3^-
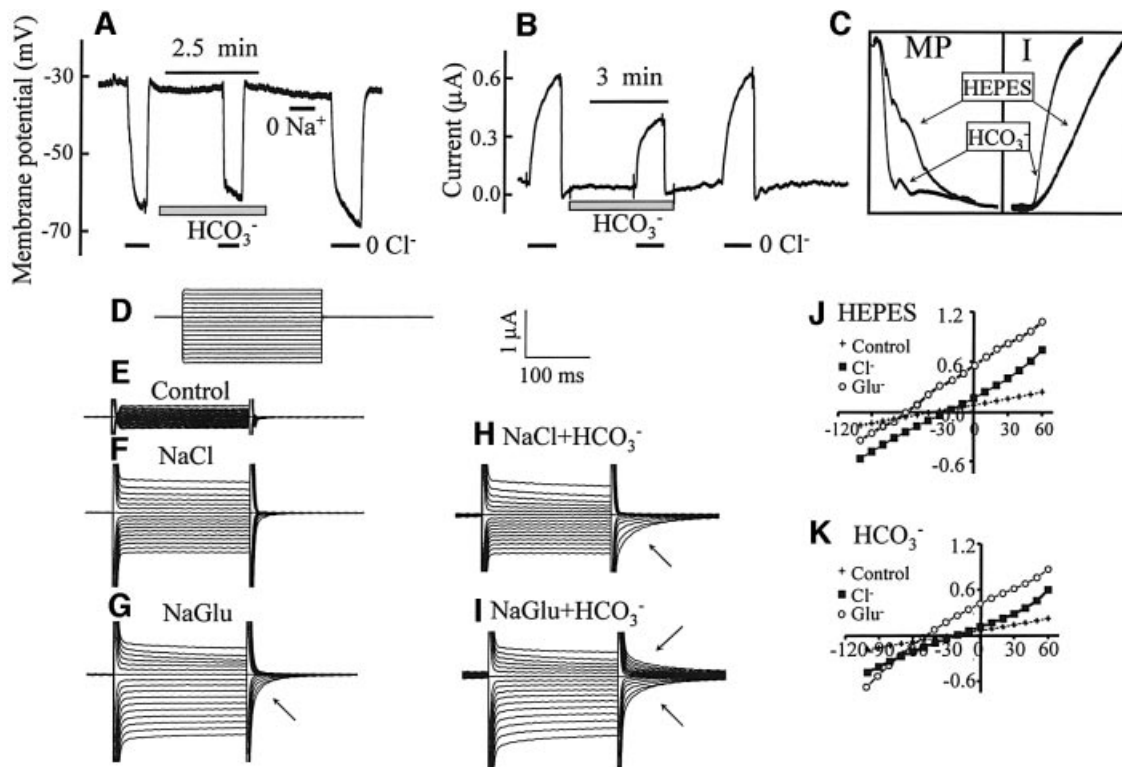
Fig. 5. Electrogenic Cl⁻ and HCO₃⁻ transport by SLC26A6. Oocytes expressing SLC26A6 were used to measure MP (**A** and **C**), current (**B** and C) or *I–V* relationships (**D–H**). The *I–V* protocol (**D**) was the same as that in Figure 4. As indicated by the bars, the oocytes were incubated in Cl⁻-free or Na⁺-free solutions in the absence or presence of HCO₃⁻. Current was measured at a holding MP of –30 mV. (C) The effect of HCO₃⁻ on the rates of changes in MP (left) and current (right) in an expanded time scale. Small arrows next to traces in (G–I) point to tail currents.

transport by DRA and SLC26A6 expressed in *Xenopus* oocytes. Completely unexpectedly, we found that these transporters are electrogenic, with unique properties. Shown in Figure 4 is a partial characterization of Cl⁻ and HCO₃⁻ transport by DRA. The membrane potential (MP) of water-injected oocytes bathed in HEPES-buffered media was -47 ± 5 mV ($n = 39$). Removal of external Cl⁻ or Na⁺ caused a small membrane hyperpolarization in control cells (Figure 4A). Expression of DRA decreased the MP to -26 ± 4 mV ($n = 19$). Figure 4C shows that removal of Cl⁻ depolarized the MP by 15 ± 5 mV ($n = 13$). Addition of HCO₃⁻ in the presence of Cl⁻ depolarized the MP by 3 ± 2 mV ($n = 9$) and largely prevented the depolarization due to removal of Cl⁻ caused by a shift in the reversal potential (RP; see below).
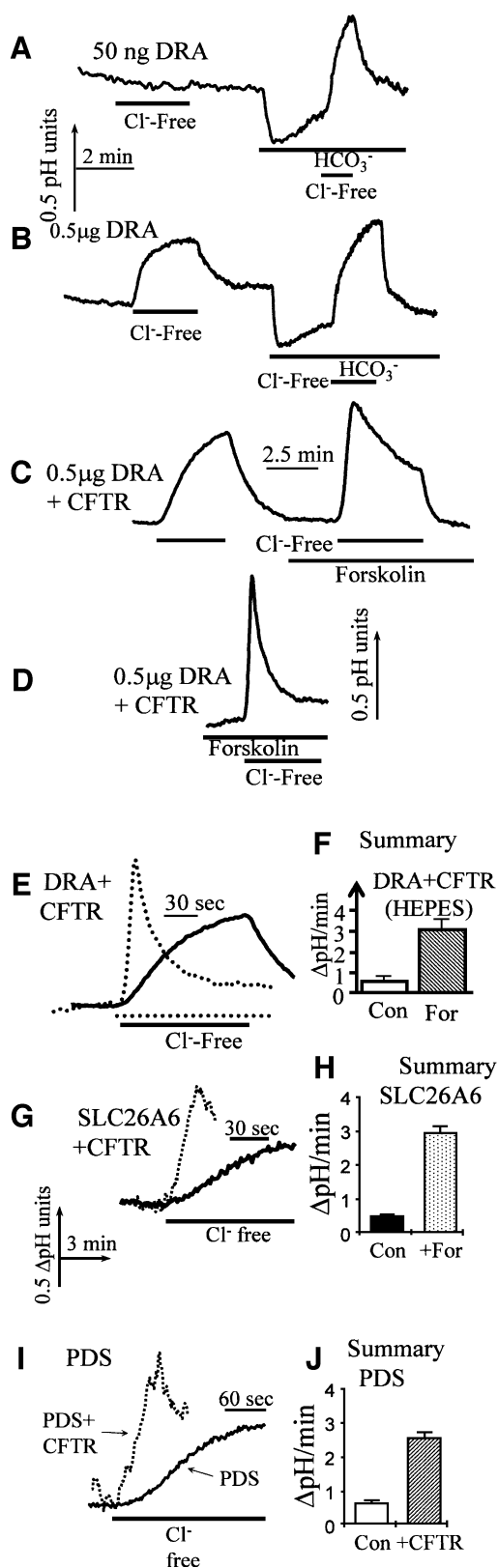
Figure 4B shows measurement of current in control, water-injected oocytes, and Figure 4D shows the current measures in DRA-expressing oocytes. The MP was held at -30 mV and every 10 s stepped to ± 60 mV for 0.5 s. It is evident that expression of DRA induced an outwardly rectifying current. Stepping the MP of oocytes to +60 mV in NaCl medium resulted in an outward current of 0.89 ± 0.13 μA ($n = 7$), which was markedly reduced upon removal of Cl⁻. Addition of HCO₃⁻ reduced the outward current by 0.16 ± 0.05 μA ($n = 7$), which was reduced by removal of Cl⁻ to the level measured in the absence of HCO₃⁻. Cl⁻/HCO₃⁻ exchange by DRA is not inhibited by DIDS (Melvin *et al.*, 1999) whereas the endogenous outwardly rectifying Cl⁻ current is completely inhibited by 0.1 mM DIDS (Schmieder *et al.*, 1998). Therefore, we tested the effect of DIDS on the current in

control and DRA-expressing oocytes (Figure 4B and D). DIDS had minimal effect in water-injected oocytes and inhibited the current in DRA-expressing oocytes by only 0.13 ± 0.03 μA ($n = 5$).

An important effect of HCO₃⁻ is shown in Figure 4E and F. Although it reduced the Cl⁻-dependent current, HCO₃⁻ increased the rates of current changes due to Cl⁻ removal and addition by $39 \pm 5\%$ ($n = 7$, $P < 0.01$). This suggests that HCO₃⁻ coupling to Cl⁻ transport is better than OH⁻ coupling. Another effect of HCO₃⁻ is revealed in the *I–V* plots (Figure 4G and H). In a Cl⁻ solution, the current had an RP of -38 ± 5 mV ($n = 7$). As expected, removal of Cl⁻ inhibited mainly the outward current and shifted the RP to -12 ± 3 mV ($n = 7$). HCO₃⁻ reduced the outward and inward currents and shifted the RP in the presence of Cl⁻ to -27 ± 4 mV ($n = 7$).

Several conclusions emerge from the findings in Figure 4. First, although the results are not sufficient to determine the mode of transport with certainty, it is likely that Cl⁻ and OH⁻/HCO₃⁻ transport is coupled, at least in part, since HCO₃⁻ accelerated the rates of current changes due to Cl⁻ removal and shifted the RP in the positive direction. Secondly, depolarization due to Cl⁻ removal can be explained if the coupling stoichiometry of DRA is Cl⁻/OH⁻–HCO₃⁻ $\geqslant 2$. Thirdly, inhibition of the inward current by HCO₃⁻ suggests that accumulation of intracellular HCO₃⁻ inhibits the Cl⁻$_{in}$/HCO₃⁻$_{out}$ (reverse mode) exchange. This has the physiological advantage of positioning DRA to function only in the forward direction of Cl⁻$_{out}$/HCO₃⁻$_{in}$ exchange and prevent leakage when [HCO₃⁻] in the ductal fluid reaches high concentrations.

These combined properties make DRA an ideal concentrator of HCO_3^- in secretory fluids. Thus, DRA in the distal portion of the ductal system of secretory epithelia can absorb all the residual Cl^- while concentrating HCO_3^- to >140 mM.

Fig. 6. Activation of DRA by CFTR. Cells were transfected with 50 ng (**A**) or 0.5 μg of DRA (**B**), or 0.5 μg of DRA and 1.5 μg of CFTR (**C** and **D**). Cells were perfused with HEPES-buffered solutions to evaluate Cl^-/OH^- exchange and then with HCO_3^--buffered solutions to measure Cl^-/HCO_3^- exchange. Cl^-/OH^- and Cl^-/HCO_3^- exchange were estimated from the changes in pH_i due to the removal and addition of Cl^-, as indicated by the bars in each experiment. Where indicated, the cells were also stimulated with forskolin. Note that stimulation of CFTR was obligatory for activation of DRA (C and D). The first portion of the experiments in (C) and (D) is illustrated in (**E**). (**F**) A summary of the results of 11 (DRA only) and 17 (DRA + CFTR) experiments. (**G–J**) The effect of CFTR on Cl^-/OH^- exchange by SLC26A6 and PDS, respectively. The average of four experiments under each condition is presented.

The second member of the SLC26 family analyzed is SLC26A6, and the results obtained with this transporter are illustrated in Figure 5. Remarkably, SLC26A6 shows many properties opposite to those of DRA. Thus, the MP of oocytes expressing SLC26A6 was -34 ± 3 mV($n = 33$). Removal of Cl^- hyperpolarized the oocytes to -62 ± 7 mV ($n = 9$), while generating an outward current of 0.6 ± 0.1 μA ($n = 9$) at an MP of -30 mV (Figure 5A and B). Removal of Na^+ had no effect on the MP or current. Addition of HCO_3^- did not change the MP, but markedly increased the rate of MP and current changes due to removal of Cl^- by 3.63 ± 0.27-fold, $n = 6$ (Figure 5C), similar to findings with DRA. The small Cl^--dependent currents may reflect the broad substrate specificity of SLC26A6, which transports molecules as large as formate (Knauf *et al.*, 2001) and oxalate (Jiang *et al.*, 2002), and thus may have only a small preference for Cl^- over gluconate. This is also reflected in the finding that the *I–V* plots in the presence and absence of Cl^- are similar, but with different RPs. The RP in the presence of Cl^- was -25 ± 3 mV ($n = 7$) and shifted to -51 ± 6 mV ($n = 7$) in the absence of Cl^-. Examination of the *I–V* traces showed that the current slowly inactivated at an MP above the RP and the inactivation was accelerated by HCO_3^-. Current inactivation resulted in tail currents upon return to the holding MP (Figure 5H). Removal of Cl^- in the absence of HCO_3^- accelerated inactivation only at positive MP, but removal of Cl^- in the presence of HCO_3^- resulted in voltage-dependent current inactivation and tail currents in both directions. Interestingly, in the presence of HCO_3^-, the current showed shallow outward rectification.

The important conclusions from these findings are (i) Cl^- and HCO_3^- transport by SLC26A6 are probably well coupled, as suggested by stimulation of the rates of MP and current changes due to Cl^- removal; (ii) the Cl^-/HCO_3^- stoichiometry of SLC26A6 is opposite to that of DRA and must be $HCO_3^-/Cl^- \geqslant 2$; and (iii) transport by SLC26A6 is regulated by voltage. These properties make SLC26A6 an excellent Cl^--absorbing transporter. We also note that expression of two members of the SLC26 family in the same cell (and in the case of epithelia, in the same membrane domain), one with the Cl^-/HCO_3^- stoichiometry of DRA and one with that of SLC26A6, results in an apparent electroneutral Cl^-/HCO_3^- exchange.

CFTR activates SLC26 transporters

Transport of Cl^- and HCO_3^- by the SLC26 transporters prompted us to test the effect of CFTR on the activity of these transporters. This could not be accomplished reliably
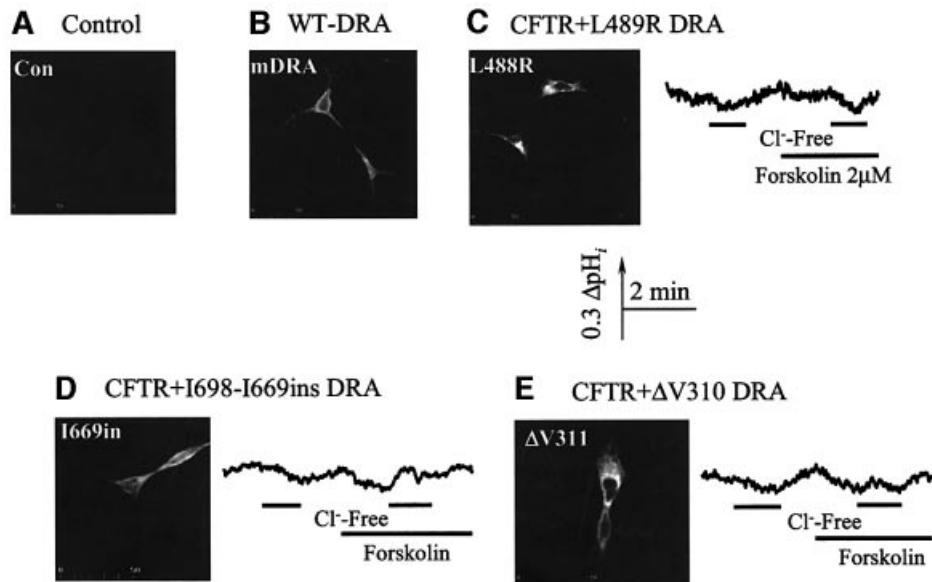
Fig. 7. Active DRA is essential for CFTR stimulated Cl⁻/OH⁻ exchange. HEK 293 cells were transfected with wild-type or the indicated mutants of DRA and used for immunolocalization. (**A**) Control with cells transfected with GFP. Note that wild-type (**B**), L489R (**C**) and I668–669ins (**D**) were expressed in the plasma membrane, whereas ΔV310 (**E**) was retained in the endoplasmic reticulum and is used as a control. When expressed alone or together with CFTR, none of the mutants showed any Cl⁻/OH⁻ exchange activity.
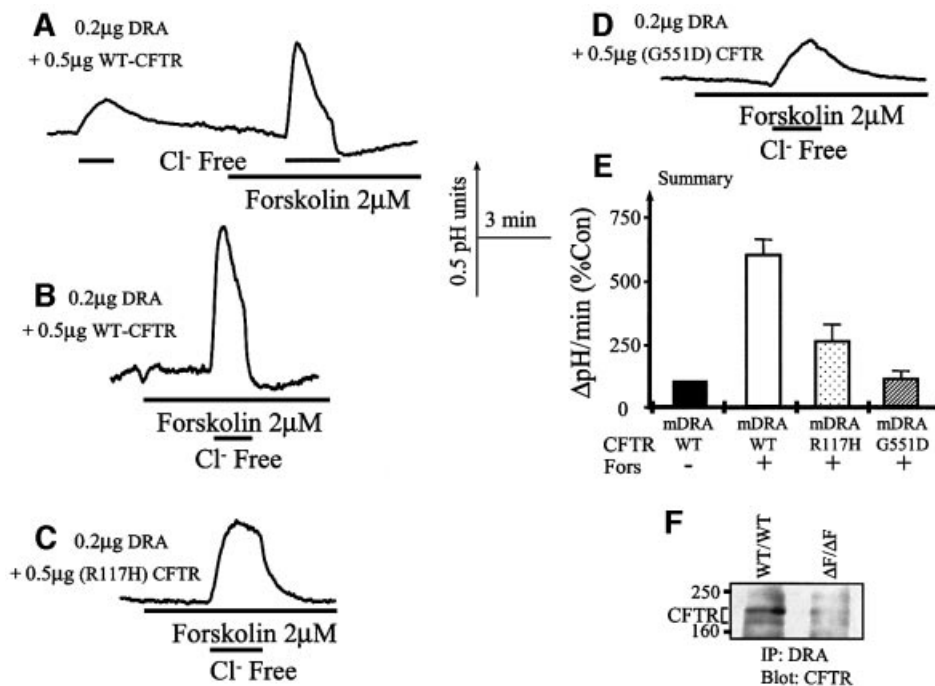

Fig. 8. Interaction between CFTR and mutants with DRA *in vitro* and *in vivo*. HEK 293 cells were transfected with low levels of DRA and the indicated CFTR constructs. Cells from each group were stimulated before measurement of Cl⁻/OH⁻ exchange. All cells were transfected with 0.2 μg of DRA. In (**A**) and (**B**), the cells were transfected with 0.5 μg of CFTR, in (**C**) with 0.5 μg of CFTR(R117H) and in (**D**) with 0.5 μg of CFTR(G551D). (**E**) Summary of the results of four to seven experiments under each condition. In (**F**), pancreatic extract was used to immunoprecipitate DRA and the immunoprecipitate was blotted for CFTR.

by current measurement since all transporters are electrogenic and generate a Cl⁻ current. Therefore, for these experiments, we resorted to pH_i measurements and took advantage of the Cl⁻/OH⁻ exchange mediated by the SLC26 transporters, as we did with the AEs (Figure 3). This is illustrated in Figure 6 for DRA, SLC26A6 and PDS. The entire protocols for SLC26A6 and PDS can be found in the Supplementary data available at *The EMBO Journal* Online. Figure 6A shows that expression of a low level of DRA had a minimal effect on Cl⁻/OH⁻, but increased Cl⁻/HCO₃⁻ exchange. At higher levels of DRA, the Cl⁻/OH⁻ exchange could be observed (Figure 6B). The behavior described in Figure 6A and B was observed in all experiments tested (>150) and reflects the ability of

members of the family to transport OH^-, but to transport HCO_3^- better than OH^-.

Since expression of CFTR never activated Cl^-/OH^- exchange and the effect of CFTR was dependent on stimulation with forskolin, we could study regulation of DRA and other members of the SLC26 family by following Cl^-/OH^- exchange. Figure 6C shows that co-expression of CFTR and DRA had no effect on Cl^-/OH^- exchange prior to cell stimulation. Subsequent stimulation of CFTR resulted in a much faster rate of Cl^-/OH^- exchange (second part of Figure 6C). Figure 6D and E shows that an even more dramatic effect of CFTR on Cl^-/OH^- exchange was observed if the cells were stimulated with forskolin before the first removal of $[Cl^-]_o$. The summary in Figure 6F shows that CFTR increased DRA-mediated Cl^-/OH^- exchange by ~6-fold ($n = 13$). Activation of DRA by CFTR was also observed in HCO_3^--buffered media, but the rate of the Cl^-/HCO_3^- exchange was too fast to allow reliable quantification, even at low level expression of the proteins. Another notable finding in Figure 6C–E is that the pH_i changes due to removal of Cl^- were stable in the absence of CFTR, but transient in stimulated cells expressing DRA and CFTR. The same behavior was observed with all members of the family (see below).

DRA and PDS show relatively limited tissue distribution (Schweinfest et al., 1993; Everett et al., 1997; Wheat et al., 2000; Wang et al., 2002). In contrast, the northern dot blot in Supplementary figure 1A demonstrates wide expression of SLC26A6, with high levels of mRNA in the pancreas, intestine, colon and lung, all tissues that express high levels of CFTR. The other traces in Supplementary figure 1 are controls demonstrating that when stably expressed in HEK 293 cells, SLC26A6 functions as a Cl^-/OH^- and Cl^-/HCO_3^- exchanger. Notably, Figure 6G and H shows that SLC26A6-mediated anion exchange is activated 6-fold by CFTR. Again, under these conditions, the pH_i change was transient. Experiments similar to those with DRA and SLC26A6 were performed with PDS, and the controls are shown in Supplementary figure 2. Figure 6I and J shows that CFTR activates PDS-mediated Cl^-/OH^- exchange by ~5-fold. Hence, it is clear that CFTR activates all members of the SLC26 family tested. As will be argued below, this can account for all forms of CFTR-stimulated HCO_3^- transport in epithelia.

We do not know at present the reason for the transient change in pH_i observed when CFTR-stimulated SLC26A6 members are exposed to Cl^--free media. However, to show that the entire profile of pH_i change requires active DRA and that activation of DRA by CFTR may have significance beyond CF, we evaluated the effect of mutations in DRA that cause congenital chloride diarrhea (CLD) (Hoglund et al., 1998) on the ability of DRA to transport OH^- and the ability of CFTR to stimulate DRA. The L489R, I668–669ins mutants of DRA are expressed in the plasma membrane (Figure 7C and D) and the $\Delta V310$ mutant was retained in the endoplasmic reticulum (Figure 7E). None of the disease-associated DRA mutants mediated Cl^-/OH^- or Cl^-/HCO_3^- exchange. Furthermore, co-expression of the mutants with CFTR did not rescue exchange activity, indicating that functional DRA was needed to observe the transient change in pH_i in cells

expressing DRA and CFTR. Finally, the activity of DRA is not inhibited by DIDS (Melvin et al., 1999) and continued so after activation by CFTR, whereas the activities of PDS (Soleimani et al., 2001) and SLC26A6 (S.B.H.Ko and S.Muallem, unpublished data) are DIDS inhibitable and remained so after stimulation by CFTR.

Relevance to CF
In a previous work, we reported that several CF-associated mutants in CFTR show aberrant activation of HCO_3^- transport (Choi et al., 2001). Therefore, we tested the ability of selective CFTR mutants to activate DRA as a representative of the SLC26 family. We focused on the R117H and the G551D mutants since these mutants are well characterized clinically and R117H is associated with a mild form and G551D with a severe form of CF (Wilschanski et al., 1995). For these experiments, the cells were transfected with a reduced amount of cDNA to avoid masking the effect of the mutants due to overexpression. Figure 8A, B and E shows that at the lower expression levels, CFTR still activates DRA by ~6-fold. Figure 8C and E shows that the R117H mutant activated DRA by only 2.5-fold (26% of that by the wild-type CFTR), whereas the G551D mutant was unable to activate DRA.

For CFTR to regulate members of the SLC26 family, they need to exist in the same HCO_3^--transporting complex. Figure 8F shows that immunoprecipitation of DRA from the pancreas co-immunoprecipitated CFTR from wild-type, but not $\Delta F/\Delta F$ mice. This finding further supports a physiological significance for the regulation of SLC26 transporters by CFTR.

The findings reported here can explain many previous observations and have significant implications for the molecular mechanism of epithelial HCO_3^- secretion, CF and CLD. Our previous findings (Lee et al., 1999a) and the results in Figure 1 suggested that CFTR activates an electroneutral Cl^--dependent HCO_3^- transport with close to a 1:1 stoichiometry. Yet, we exclude the SLC4 and identify the electrogenic SLC26 transporters as the Cl^- and HCO_3^- transporters activated by CFTR. The most likely explanation can be found in the properties of the SLC26s. Measurement of pH_i and current showed that all members of the family examined transport Cl^- and HCO_3^-, and the transport is probably coupled. Most importantly, the stoichiometry of the transport is isoform specific. Hence, while DRA couples the transport of 1 HCO_3^- to at least 2 Cl^-, SLC26A6 couples the transport of 1 Cl^- to at least 2 HCO_3^-. Expression of two transporters with opposite stoichiometry will result in an apparent electroneutral Cl^-/HCO_3^- exchange. To date, nine members of the SLC26 family have been identified, each of which is likely to have several splice variants. It is thus conceivable that two transporters will be expressed in the same cell. Indeed, preliminary RT–PCR analysis revealed expression of at least two SLC26 members in native secretory cells and HEK 293 cells. Once all members of the SLC26 family and their properties are known, it will be informative to perform extensive analysis of these transporters in HEK 293 and other epithelial cells.

It is generally assumed that CFTR itself mediates the electrogenic portion of HCO_3^- secretion. However, CFTR is a poor transporter of HCO_3^-, and the results in Figures 1 and 2 show that CFTR-mediated HCO_3^- current cannot

account for HCO_3^- fluxes measured under the same conditions. Activation of the SLC26s by CFTR removes the need to assume that CFTR mediates the electrogenic portion of epithelial HCO_3^- secretion. The transport properties of the SLC26s and their activation by CFTR can explain all forms of epithelial HCO_3^- secretion. Thus, domination of one of the SLC26 transporters in a cell type or tissue and its activation by CFTR, such as DRA in the colon, can account for the electrogenic component of HCO_3^- transport. Expression of two SLC26s in one cell/tissue can account for the electroneutral component. It is of note that CFTR activates the SLC26s by 5- to 6-fold. This may be viewed as a switching mechanism in which CFTR can turn HCO_3^- transport on or off in the various CFTR-expressing cells.

Another important implication of our findings is that we can finally explain in molecular terms how the pancreatic, salivary and possibly other ductal systems secrete a fluid containing ~20 mM Cl^- and 140 mM HCO_3^-. Expression of an SLC26 isoform with the properties of SLC26A6 in the proximal portion of the duct will make efficient use of the Cl^- gradient to secrete HCO_3^-. However at $[Cl^-]_i$ of 10–15 mM (Ishiguro *et al.*, 2002) and a HCO_3^-/Cl^- stoichiometry of ≥ 2, the maximal $[HCO_3^-]$ in the secreted fluid generated by such a transporter cannot exceed 40–60 mM. The advantage of a transporter with a HCO_3^-/Cl^- stoichiometry of ≥ 2 is that it removes the need for circulation of Cl^- by CFTR to allow the net absorption of 40 mM Cl^- by this portion of the duct. Expression of an SLC26 isoform with the properties of DRA in a distal portion of the duct having a Cl^-/HCO_3^- stoichiometry of ≥ 2 can reduce Cl^- to 20 mM and increase HCO_3^- to >140 mM in the secreted fluid. A unique feature of DRA that supports such a role is the outward rectification and inhibition of reverse Cl^-/HCO_3^- exchange by internal HCO_3^-. This makes transport by DRA practically unidirectional, HCO_3^- secretion and Cl^- absorption, to prevent HCO_3^- leakage. Furthermore, DRA can be activated by depolarization of the luminal membrane, precisely what happens upon activation of CFTR. Hence, we believe that our findings solve a long-standing puzzle in epithelial/pancreatic HCO_3^- secretion of how ducts can generate a fluid containing 20 mM Cl^- and 140 mM HCO_3^-.

A significant finding was the modified activation of DRA by the R117H and G551D mutants of CFTR. As representative of CFTR mutants associated with CF, the findings with these mutants indicate that mutations in CFTR affect at least two functions of CFTR; Cl^- channel activity and regulation of the SLC26 transporters. Furthermore, our previous work showed that loss of ability to activate HCO_3^- transport is more sensitive to mutations in CFTR than is Cl^- channel activity (Choi *et al.*, 2001). This implies that the two activities are separate functions of CFTR. Hence, the current findings provide a molecular mechanism for the aberrant HCO_3^- transport in CF. Furthermore, we note that members of the SLC26 family with the properties of DRA, by absorbing 2 Cl^- in exchange for HCO_3^-, perform net absorption of osmolites and can reduce the osmolarity of the secreted fluid. As such, altered activation of these transporters by CFTR will contribute to the problem of increased osmolarity of the secreted fluid, which may be of critical significance in the lung. Accordingly, increased expression and/or activation of DRA-type transporters can be an alternative approach to reduce the symptoms of CF. This approach can be very attractive if expression of DRA-like transporters is normal in CF tissues.

Materials and methods

CFTR, mDRA, AE1-3, hPDS and cRNA
pCMVNot6.2/CFTR was provided by Dr J.Rommens (The Hospital for Sick Children). The R117H and G551D mutants were prepared as described (Choi *et al.*, 2001). pClneo/mDRA was a gift from Dr J.Melvin (University of Rochester), pClneo/hPDS from Dr M.Soleimani (University of Cincinnati) and the AE1–3 constructs from Dr R.Kopito (Stanford University). cRNA was prepared by linearizing pcDNA3/CFTR (a gift from Dr K.Kirk, University of Alabama) with *Xho*I. The cRNA was transcribed using a T7 RNA polymerase kit, purified by phenol/chloroform precipitation and dissolved in nuclease-free water.

Preparation of the pCMVHA/mDRA construct
To prepare hemagglutinin (HA)-tagged mDAR, cDNA with *Xho*I and *Not*I on both ends was generated by PCR with the primers: sense 5′-TCTCTCGAGGTATGATCGAAGCCATAGGG-3′ and antisense 5′-TTAAGCGGCCGCAGATGAGAATCCTTCCGAATTG-3′. The PCR product was excised and ligated into pCMVHA. Five colonies were selected and verified by sequencing to have an HA tag at the N-terminus. All clones retained anion exchange activity when expressed in HEK 293 cells. Mutations were introduced into the pClneo/ or pCMVHA/mDRA using the Quickchange kit. The primers used are: ΔV310, sense 5′-GGTTTGGCGTGGCCGTGGGGAACATGAGTCTTGG-3′, antisense 5′-CCAAGACTCATGTTCCCCACGGCCACGCCAAACC-3′; L489R, sense 5′-GCAAGTGTAGCATTTCAACGCCTAACTATTGTGTTCA-GGACC-3′, antisense 5′-GGTCCTGAACACAATAGTTAGGCGTTG-AAATGCTACACTTGC-3′; I668–669ins sense, 5′-GCCTCAGAAC-GATTTTACAAGAATTTATTATCAGGATCAAGGTGG-3′, antisense, 5′-CCACCTTGATCCTGATAATAAATTCTTGTAAAATCGTTCTG-AGGC-3′. At least four positive colonies from each mutant were selected, and incorporation of the mutations was verified by sequencing.

Preparation of rat AE4 and SLC26A6
The AE4 construct in pCMV-SPORT was prepared as described before (Ko *et al.*, 2002). To prepare SLC26A6, a human expressed sequence tag (EST) clone (DDBJ/EMBL/GenBank accession No. AL036079) was identified by a BLAST search using the reported SLC26A6 sequence (AF279265) as a query. The EST clone was obtained from RZPD (Germany) and sequenced. The *Sal*I and *Not*I sites were used to excise the coding region and ligate it into pcDNA3.1.

Expression of SLC26A6 in human tissues
Multiple tissue RNA blot (human RNA master blot, 7770-1, Clontech) was hybridized under high stringency with the SLC26A6 cDNA labeled with $[\alpha\text{-}^{32}P]dCTP$.

Expression in HEK 293 cells
HEK 293 cells were cultured in Dulbecco's modified Eagle's medium-high glucose supplemented with 10% fetal calf serum, penicillin (100 U/ml) and streptomycin (100 μg/ml), and plated on glass coverslips. Various amounts of CFTR and/or mDRA plasmids were co-transfected with 1.5 μg of a green fluorescent protein (GFP)-containing plasmid (pCMVGFP) using Lipofectamine. Cells were used 48–72 h post-transfection. To prepare cells stably transfected with PDS and SLC26A6, HEK 293 cells were grown on 35 mm dishes and transfected with 3 μg of the plasmid of interest. Expression of the proteins was verified by gain of Cl^-/OH^- exchange activity.

Immunocytochemistry and immunoprecipitation
HEK 293 cells were transfected with wild-type and mutant HA-mDRA. After 48 h, the cells were washed with phosphate-buffered saline (PBS), fixed with 4% formaldehyde and permeabilized with 0.1% Triton X-100 in PBS for 10 min. After fixation, immunostaining was performed as described before (Lee *et al.*, 1999a). Anti-HA antibody was used at a 1:1000 dilution and images were collected with a Bio-Rad 1020. For immunoprecipitation, anti-DRA antibodies were raised in rabbits against the C-terminal sequence INTNGGLRNRECQVPVETKF. Anti-CFTR

antibodies were purchased from R&D. Pancreatic extracts were incubated with a 1:2000 dilution of anti-DRA and protein A–Sepharose beads over night. The beads were collected, washed and proteins were released by heating at 37°C for 1 h. The released proteins were blotted for CFTR.

pH_i and $[Cl^-]_i$ measurements

pH_i and $[Cl^-]_i$ were measured as previously detailed (Lee *et al.*, 1999a,b). In brief, glass coverslips with cells attached to them formed the bottom of a perfusion chamber. The cells were washed with a HEPES-buffered solution A containing 140 mM NaCl, 5 mM KCl, 1 mM MgCl$_2$, 1 mM CaCl$_2$, 10 mM glucose and 10 mM HEPES (pH 7.4 with NaOH). The level of transfection was estimated from GFP fluorescence, which was used to normalize Cl$^-$ and HCO$_3^-$ transport rates in each set of experiments. Cells were loaded with BCECF by a 10 min incubation at room temperature in solution A containing 2.5 μM BCECF-AM. BCECF fluorescence was measured from 1–3 cell clusters by photon counting using the conditions described before (Lee *et al.*, 1999a). HCO$_3^-$-buffered solutions were prepared by replacing 25 mM Cl$^-$ or gluconate salt with 25 mM HCO$_3^-$ and continuously gassing with 95% O$_2$ and 5% CO$_2$. Cl$^-$-free solutions were prepared by replacing Cl$^-$ with gluconate. High K$^+$ solutions were prepared by replacing between 100 and 140 mM NaCl with KCl. When desired, forskolin was added to the perfusate from a stock solution of 10 mM in dimethylsulfoxide (DMSO). BCECF fluorescence was recorded at excitation wavelengths of 490 and 440 nm at a resolution of 2/s.

For $[Cl^-]_i$ measurements, the cells were loaded with MQAE by 2 h incubation at 37°C in solution A containing 5 mM MQAE. After mounting, the cells were washed and MQAE fluorescence was recorded from a GFP-expressing cell at an excitation wavelength of 360 nm. To measure Cl$^-$ permeability, the cells were exposed to NO$_3^-$-containing solution, which was prepared in the same way as solution A but replacing all Cl$^-$ salts with equivalent NO$_3^-$ salts. To measure HCO$_3^-$-dependent Cl$^-$ transport, the cells were incubated with HCO$_3^-$-buffered solutions.

Calibration of pH_i and $[Cl^-]_i$

Calibration of BCECF fluorescence in the cells was performed as before (Lee *et al.*, 1999a), using the high K$^+$, nigericin (Nig) technique. To calculate HCO$_3^-$ fluxes, changes in pH_i were converted to changes in [HCO$_3^-$] by measuring buffer capacity (Muallem and Loessberg, 1990) and using the equations $\beta i = \Delta[NH_4^+]_{in}/\Delta pHi$ and $\beta t = \beta i + 2.3[HCO_3^-]_{in}$, where βi is the buffer capacity in HEPES-buffered media and βt is the total buffer capacity in HCO$_3^-$-buffered media. Dependence of βi on pH_i was determined by acidifying the cells with an NH$_4^+$ pulse and incubation in Na$^+$-free, HEPES-buffered solution. The cells were then exposed to the same solution containing between 2.5 and 40 mM NH$_4^+$. βi decreased nearly linearly as pH_i increased from 6.5 to 7.4. βt was calculated to be nearly constant between a pH_i of 6.5 and 7.3 (for details see Muallem and Loessberg, 1990) and averaged 41.3 ± 3.6 mM HCO$_3^-$/pH unit ($n = 5$). To calculate Cl$^-$ fluxes, the MQAE signals were calibrated by measuring a Stern–Volmer constant for MQAE in HEK 293 cells of 14.5 ± 1.1/M ($n = 5$). For this measurement, the cells were bathed in 145 mM K$^+$ solutions containing between 0 and 100 mM Cl$^-$, 2.5 μM Nig and 10 μM tributyltin (TBT) with pH set at 7.3 to clamp intracellular pHi and $[Cl^-]_i$ at the desired concentrations (Zhao and Muallem, 1995). The constant was used to determine $[Cl^-]_i$ in resting HEK 293 cells bathed in HEPES-buffered solution A as 35 ± 4 mM. This value and a two-point procedure were used to calculate the rate and/or extent of Cl$^-$ fluxes in the experiments. Thus, exposure of stimulated, CFTR-expressing cells to NO$_3^-$ resulted in complete exchange of Cl$^-$ with NO$_3^-$ and a maximal unquenching of MQAE fluorescence. This change in fluorescence was taken as representing a 35 mM change in $[Cl^-]_i$, and all other changes were calculated based on this calibration.

Current measurements

Oocytes were obtained by partial ovariectomy of female *Xenopus laevis* anesthetized with 2 g/l methanesulfonate-3-aminobenzoic acid ethyl ester. Folliculated cells were removed into Ca^{2+}-free OR-2 medium composed of 82.5 mM NaCl, 2.4 mM KCl, 1 mM MgCl$_2$, 5 mM HEPES-Na pH 7.5 containing 1 mg/ml collagenase B. De-folliculated oocytes were washed 4–5 times with Ca^{2+}-free OR-2. Healthy oocytes in stages V–VI were maintained at 18°C in ND96 medium composed of 96 mM NaCl, 2 mM KCl, 1.8 mM CaCl$_2$, 1 mM MgCl$_2$, 2.5 mM Na$^+$-pyruvate, 5 mM HEPES-Na pH 7.5, 100 μg/ml streptomycin and 100 U/ml penicillin. Oocytes were injected with 10–50 ng of cRNA of the various clones in a final volume of 50 nl using a manual injector, and incubated at 18°C in ND96. The medium was changed every day, and oocytes were assayed 48–96 h post-injection. Voltage and current recordings were accomplished with the two-electrode voltage-clamp procedure using an OC-725C Oocyte Clamp System. Electrodes were filled with 3 M KCl and had resistances of 0.5–2 MΩ. CFTR was activated by 10 μM forskolin and 100 μM 3-isobutyl-1-methylxantine (IBMX). The current and voltage of DRA and SLC26A6 were recorded in unstimulated oocytes. Currents were digitized and analyzed using an AxoScope 8.1 system and a Digi-data 1322A AC/DC converter.

For HEK cells, the whole-cell mode of the patch–clamp technique was used. The pipet solution contained 35 mM NMDG-Cl, 110 mM NMDG-gluconate, 2 mM EGTA, 3 mM MgSO$_4$, 5 mM Tris-ATP and 10 mM HEPES pH 7.3. After establishing the whole-cell configuration, the bath solution was changed to a solution containing 145 mM NMDG-Cl$^-$, 2 mM EGTA and 10 mM HEPES pH 7.4. The cells were stimulated with forskolin before or after reducing bath Cl$^-$ to either 1 or 3.5 mM by replacing Cl$^-$ with gluconate in the bath solution. To evaluate the HCO$_3^-$ current, stimulated cells incubated in solutions containing 1 or 3.5 mM Cl$^-$ were exposed to the NMDG-gluconate bath solution in which 25 mM choline-HCO$_3$ replaced 25 mM NMDG-gluconate and were gassed with 5%CO$_2$/95% O$_2$. The cells were held at –60 mV throughout. The patch clamp output was filtered at 20 Hz. Recording was performed with pClamp 6 and a Digi-Data 1200 interface.

Statistical analysis

Results in all experiments are given as the mean ± SEM of the indicated number of experiments. The results of multiple experiments were analyzed using paired or non-paired Student's *t*-test as appropriate.

Supplementary data

Supplementary data are available at *The EMBO Journal* Online.

References

Alper,S.L. (1991) The band 3-related anion exchanger (AE) gene family. *Annu. Rev. Physiol.*, **53**, 549–564.

Argent,B.E. and Case,R.M. (1994) Cellular mechanisms and control of HCO$_3^-$ secretion. In Johnson,L.R. (ed.), *Textbook of Physiology of the Gastrointestinal Tract*, 3rd edn. Raven Press, New York, NY, pp. 1478–1498.

Choi,J.Y., Muallem,D., Kiselyov,K., Lee,M.G., Thomas,P.J. and Muallem,S. (2001) Aberrant CFTR-dependent HCO$_3^-$ transport in mutations associated with cystic fibrosis. *Nature*, **410**, 94–97.

Cook,D.I., Van Lennep,E.W., Roberts,M.L. and Young,J.A. (1994) Secretion by the major salivary glands. In Johnson,L.R. (ed.), *Textbook of Physiology of the Gastrointestinal Tract*, 3rd edn. Raven Press, New York, NY, pp. 1061–1117.

Everett,L.A. *et al.* (1997) Pendred syndrome is caused by mutations in a putative sulphate transporter gene (PDS). *Nat. Genet.*, **17**, 411–422.

Hoglund,P. *et al.* (1998) Genetic background of congenital chloride diarrhea in high-incidence populations: Finland, Poland and Saudi Arabia and Kuwait. *Am. J. Hum. Genet.*, **63**, 760–768.

Ishiguro,H., Naruse,S., Kitagawa,M., Mabuchi,T., Kondo,T., Hayakawa,T., Case,R.M. and Steward,M.C. (2002) Chloride transport in microperfused interlobular ducts isolated from guinea-pig pancreas. *J. Physiol.*, **539**, 175–189.

Jiang,Z., Grichtchenko,I.I., Boron,W.F. and Aronson,P.S. (2002) Specificity of anion exchange mediated by mouse Slc26a6. *J. Biol. Chem.*, **277**, 33963–33967.

Johansen,P.G., Anderson,C.M. and Hadorn,B. (1968) Cystic fibrosis of the pancreas. A generalised disturbance of water and electrolyte movement in exocrine tissues. *Lancet*, **1**, 455–460.

Ko,S.B.H *et al.* (2002) AE4 is a DIDS-sensitive Cl$^-$/HCO$_3^-$ exchanger in

the basolateral membrane of the renal CCD and the SMG duct. *Am. J. Physiol.*, **283**, C1206–C1219.

Kopelman,H., Corey,M., Gaskin,K., Durie,P., Weizman,Z. and Forstner,G. (1988) Impaired chloride secretion, as well as bicarbonate secretion, underlies the fluid secretory defect in the cystic fibrosis pancreas. *Gastroenterology*, **95**, 349–355.

Knauf,F., Yang,C.L., Thomson,R.B., Mentone,S.A., Giebisch,G. and Aronson,P.S. (2001) Identification of a chloride–formate exchanger expressed on the brush border membrane of renal proximal tubule cells. *Proc. Natl Acad. Sci. USA*, **98**, 9425–9430.

Kristidis,P., Bozon,D., Corey,M., Markiewicz,D., Rommens,J., Tsui,L.C. and Durie,P. (1992) Genetic determination of exocrine pancreatic function in cystic fibrosis. *Am. J. Hum. Genet.*, **50**, 1178–1184.

Lee,M.G., Wigley,W.C., Zeng,W., Noel,L.E., Marino,C.R., Thomas,P.J. and Muallem,S. (1999a) Regulation of Cl^-/HCO_3^- exchange by cystic fibrosis transmembrane conductance regulator expressed in NIH 3T3 and HEK 293 cells. *J. Biol. Chem.*, **274**, 3414–3421.

Lee,M.G., Choi,J.Y., Luo,X., Strickland,E., Thomas,P.J. and Muallem,S. (1999b) Cystic fibrosis transmembrane conductance regulator regulates luminal Cl^-/HCO_3^- exchange in mouse SMG and pancreatic ducts. *J. Biol. Chem.*, **274**, 14670–14677.

Linsdell,P., Tabcharani,J.A., Rommens,J.M., Hou,Y.X., Chang,X.B., Tsui,L.C., Riordan,J.R. and Hanrahan,J.W. (1997) Permeability of wild-type and mutant cystic fibrosis transmembrane conductance regulator chloride channels to polyatomic anions. *J. Gen. Physiol.*, **110**, 355–364.

Lohi,H., Kujala,M., Kerkela,E., Saarialho-Kere,U., Kestila,M. and Kere,J. (2000) Mapping of five new putative anion transporter genes in human and characterization of SLC26A6, a candidate gene for pancreatic anion exchanger. *Genomics*, **70**, 102–112.

Melvin,J.E., Park,K., Richardson,L., Schultheis,P.J. and Shull,G.E. (1999) Mouse down-regulated in adenoma (DRA) is an intestinal Cl^-/HCO_3^- exchanger and is up-regulated in colon of mice lacking the NHE3 Na^+/H^+ exchanger. *J. Biol. Chem.*, **274**, 22855–22861.

Moseley,R.H., Hoglund,P., Wu,G.D., Silberg,D.G., Haila,S., de la Chapelle,A., Holmberg,C. and Kere,J. (1999) Downregulated in adenoma gene encodes a chloride transporter defective in congenital chloride diarrhea. *Am. J. Physiol.*, **276**, G185–G192.

Muallem,S. and Loessberg,P.A. (1990) Intracellular pH-regulatory mechanisms in pancreatic acinar cells. I. Characterization of H^+ and HCO_3^- transporters. *J. Biol. Chem.*, **265**, 12806–12812.

O'Reilly,C.M., Winpenny,J.P., Argent,B.E. and Gray,M.A. (2000) Cystic fibrosis transmembrane conductance regulator currents in guinea pig pancreatic duct cells: inhibition by bicarbonate ions. *Gastroenterology*, **118**, 1187–1196.

Poulsen,J.H., Fischer,H., Illek,B. and Machen,T.E. (1994) Bicarbonate conductance and pH regulatory capability of cystic fibrosis transmembrane conductance regulator. *Proc. Natl Acad. Sci. USA*, **91**, 5340–5344.

Pusch,M., Jordt,S.E, Stein,V. and Jentsch,T.J. (1999) Chloride dependence of hyperpolarization-activated chloride channel gates. *J. Physiol.*, **515**, 341–353.

Quinton,P.M. (1999) Physiological basis of cystic fibrosis: a historical perspective. *Physiol. Rev.*, **79**, S3–S22.

Sabolic,I., Brown,D., Gluck,S.L. and Alper,S.L. (1997) Regulation of AE1 anion exchanger and H^+-ATPase in rat cortex by acute metabolic acidosis and alkalosis. *Kidney Int.*, **51**, 125–137.

Schmieder,S., Lindenthal,S., Banderali,U. and Ehrenfeld,J. (1998) Characterization of the putative chloride channel xClC-5 expressed in *Xenopus laevis* oocytes and comparison with endogenous chloride currents. *J. Physiol.*, **511**, 379–393.

Schweinfest,C.W., Henderson,K.W., Suster,S., Kondoh,N. and Papas,T.S. (1993) Identification of a colon mucosa gene that is down-regulated in colon adenomas and adenocarcinomas. *Proc. Natl Acad. Sci. USA*, **90**, 4166–4170.

Soleimani,M., Greenley,T., Petrovic,S., Wang,Z., Amlal,H., Kopp,P. and Burnham,C.E. (2001) Pendrin: an apical $Cl^-/OH^-/HCO3^-$ exchanger in the kidney cortex. *Am. J. Physiol.*, **280**, F356–F364.

Wang,Z., Petrovic,S., Mann,E. and Soleimani,M. (2002) Identification of an apical Cl^-/HCO_3^- exchanger in the small intestine *Am. J. Physiol.*, **282**, G573–G579.

Wheat,V.J., Shumaker,H., Burnham,C., Shull,G.E., Yankaskas,J.R. and Soleimani,M. (2000) CFTR induces the expression of DRA along with Cl^-/HCO_3^- exchange activity in tracheal epithelial cells. *Am. J. Physiol.*, **279**, C62–C71.

Wilschanski,M., Zielenski,J., Markiewicz,D., Tsui,L.C., Corey,M.,

Levison,H. and Durie,P.R. (1995) Correlation of sweat chloride concentration with classes of the cystic fibrosis transmembrane conductance regulator gene mutations. *J. Pediatr.*, **127**, 705–710.

Zhao,H. and Muallem,S. (1995) Na^+, K^+, and Cl^- transport in resting pancreatic acinar cells. *J. Gen. Physiol.*, **106**, 1225–1242.

Note added in proof

After acceptance of this manuscript Xie *et al.* (*Am. J. Physiol. Renal Physiol.*, **283**, F826–F838, 2002) reported that SLC26A6 is an electrogenic Cl^- and HCO_3^- transporter, similar to the findings in Figure 5 of the present work.